Supporting Information

A highly efficient approach to Solketal from acetone and glycerol with the supramolecular catalysis of cucurbit[6]uril

A-Min Shuai[1], Yin-Hui Huang[1], Wen-Feng Zhao[1], Qing-Mei Ge[1], Mao Liu[1], Hang Cong[1,*], Xi-Sheng Wang[1,2,*]

[1]School of Chemistry and Chemical Engineering, Guizhou University, Guiyang 550025, China

[2]Hefei National Research Center for Physical Sciences at the Microscale and Department of Chemistry, University of Science and Technology of China, Hefei 230026, China

Email: hcong@gzu.edu.cn for H. Cong

xswang77@ustc.edu.cn for X-S. Wang

Contents

1. General information

All reactions were carried out under atmospheric conditions. All reagents were commercially available and used without further purification unless otherwise stated. Cucurbit[6]uril (Q[6]) was synthesized by literature methods.[1] All reactions requiring heating were carried out using a SZCL-3A digital display intelligent temperature controlled magnetic stirrer and an oil bath.Nuclear magnetic resonance (NMR) spectra were recorded on a JEOL JNM-ECZ400S spectrometer operating at 400 MHz for proton (^{1}H), using D_2O , Chloroform-d as solvents. Chemical shifts (δ) for all ^{1}H NMR spectra were reported in parts per million (ppm). The residual solvent signals were used as references and the chemical shifts converted to the tetramethylsilane (TMS) scale (D_2O: 4.79 ppm; $CDCl_3$: 7.26 ppm for ^{1}H NMR, 77.2 ppm for ^{13}C NMR.). Gas chromatography was performed on a Shimadzu GC-2014C instrument. Electrospray Ionization Mass Spectrometry was performed on HPLC-QTOF-MS（Agilent 6545B）. The molecular structure of the catalysts was measured with a Fourier Transform Infrared Spectrometer (FTIR-ATR, affinity 1s, Shimadzu).

2. Experimental data

2.1. Comparison of Q[6] with reported catalysts in the glycerol ketalization

Table S1 Non-homogeneous catalysts for glycerol ketalization with solvent free.

Catalyst	ratio of gly. to ace.	Catalyst loading (wt% to gly.)	Temp. (◦C)	Time (h)	Conversion (%)	Solketal (%)	Ref.
ZrP-200	1:10	5	50	3	86	85	[2]
18% Fe-PKU−1	1:5	5	45	3	93	91	[3]
MOR0.5	1:10	25	60	4	99	98	[4]
UiO-SO_3H−0.2	1:10	5	60	4	70	69	[5]
BC-SO_3H−210	1:2	10	60	4	100	84	[6]
G-ASA	1:4	0.5	RT	1	97	94	[7]
$FeCl_3$/γ-Al_2O_3	1:10	0.2 mol%	25	0.5	100	98	[8]
Sulfated Modified AlMCM−41	1:10	3	25	2	99	92	[9]
MOF-808(Zr)	1:6	4	60	3	6	6	[10]
MOF-808(Hf)	1:6	4	60	3	91	89	[10]
PST−1.5	1:10	5	25	1	93	91	[11]
HPMo/AlTUD−1	1:6	10	60	3	78	73	[12]
RhMOP-SO_3H	1:4	0.5	RT	1	86	83	[13]
Co(NO_3)$_2$/γ-Al_2O_3	1:27	5.4	80	2	90	88	[14]
SO_3H-HC-MaL-B	1:5	6	70	1	98	95	[15]
Cu-FSM-16	1:2	5	60	2.5	85	77	[16]
Q[6]	1:9	3	50	0.33	100	98	This work

2.2. Catalyst recycling experiments

Table S2 Catalyst recyclability studies.

Number of cycles	Solketal (% yield)
First cycle	96.8
Second cycle	95.1
Third cycle	93.6
Fourth cycle	91.3
Fifth cycle	88.7

Reaction conditions: $n_{(gly)}$: $n_{(ace)}$ = 1:9, catalyst amount: 3 wt% $m_{(gly)}$, 50 ℃, 20 min.

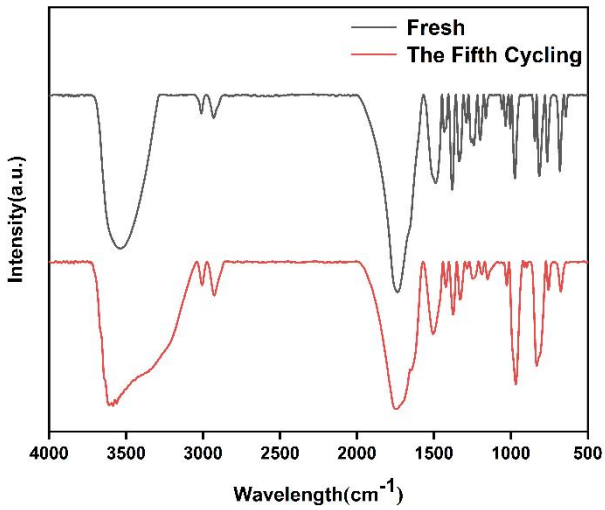

Fig. S1 FT-IR spectra of Q[6] before and after reaction.

2.3. NMR data

(2,2-dimethyl-1,3-dioxolan-4-yl)methanol (DDM): 13.52 g of colorless transparent liquid purified by flash column chromatography(n-hexane : EtOAc = 10/3), yield: 93.1%, ^{1}H NMR (400 MHz, Chloroform-d) δ 4.16 - 4.09 (m, 1H, CH), 3.94 (dd, 1H, CH_2), 3.65 - 3.70 (m, 1H, CH_2), 3.58 (dd, 1H, CH_2OH), 3.50 (dd, 1H, CH_2OH), 3.09 (br, 1H, OH), 1.34 (s, 3H, Me), 1.27 (s, 3H, Me). ^{13}C NMR (101 MHz, Chloroform-d) δ 109.39, 76.29, 65.86, 63.00, 26.67, 25.25. MS(ESI-TOF^{+}) for $C_6H_{13}O_3$ $[M+H]^+$ found 133.0867, calcd 133.0859.[17]

2,2-dimethyl-1,3-dioxan-5-ol (DDL): 0.17 g of colorless transparent liquid purified by flash column chromatography(n-hexane : EtOAc = 10/3), yield: 1.2%, ^{1}H NMR (400 MHz, Chloroform-d) δ 4.25 - 4.18 (m, 1H, CH), 4.03 - 4.01 (m, 1H, CH_2), 3.80 - 3.75 (m, 1H, CH_2), 3.73 - 3.67 (m, 2H, CH_2OH), 3.52 (br, 1H, OH), 1.45 (s, 3H, Me), 1.35 (s, 3H, Me). ^{13}C NMR (101 MHz, Chloroform-d) δ 109.46, 76.22, 65.79, 63.07, 26.76,

25.32. MS(ESI-TOF$^+$) for $C_6H_{13}O_3$ $[M+H]^+$ found 133.0865, calcd 133.0859.[18]

(2-methyl-2-propyl-1,3-dioxolan-4-yl)methanol (1a): 1.51 g of colorless transparent liquid purified by flash column chromatography(n-hexane : EtOAc = 3/1), yield: 89%, ^{1}H NMR (400 MHz, Chloroform-d) δ 4.23 - 4.10 (m, 1H, CH), 4.02-3.95 (m, 1H, CH_2), 3.74 - 3.67 (m, 1H, CH_2), 3.66-3.61 (m, 1H, CH_2OH), 3.58-3.51 (m, 1H, CH_2OH), 2.59 (br, 1H, OH), 1.63-1.52 (m, 2H, CH_2), 1.43-1.32 (m, 2H, CH_2), 1.32-1.24 (d, 3H, Me), 0.91-0.83 (td, 3H, Me). ^{13}C NMR (101 MHz, Chloroform-d) δ 111.23, 75.96, 65.89, 62.96, 41.14, 23.48, 17.25, 14.34. MS(ESI-TOF$^+$) for $C_8H_{16}O_3$ $[M+H]^+$ found 161.1172, calcd 161.1172.

(2,2-diethyl-1,3-dioxolan-4-yl)methanol (2a): 1.59 g of colorless transparent liquid purified by flash column chromatography(n-hexane : EtOAc = 3/1), yield: 92%, ^{1}H NMR (400 MHz, Chloroform-d) δ 4.13 - 4.04 (m, 1H, CH), 3.96-3.89 (m, 1H, CH_2), 3.61 - 3.43 (m, 3H, CH_2, CH_2OH), 3.17 (br, 1H, OH), 1.58-1.46 (dq, 4H, CH_2), 0.82-0.74 (td, 6H, Me). ^{13}C NMR (101 MHz, Chloroform-d) δ 113.27, 76.54, 66.43, 63.06, 29.52, 29.19, 8.14, 7.82. MS(ESI-TOF$^+$) for $C_8H_{16}O_3$ $[M+H]^+$ found 161.1170, calcd 161.1172.

(1,4-dioxaspiro[4.5]decan-2-yl)methanol (5a): 1.61 g of colorless transparent liquid purified by flash column chromatography(n-hexane : EtOAc = 5/1), yield: 86%, ^{1}H NMR (400 MHz, Chloroform-d) δ 1.47 - 1.60 (m, 2H, CH_2), 1.61 - 1.80 (m, 8H, CH_2), 3.41 - 3.45 (br, 1H, OH), 3.67 - 3.81 (m, 4H, CH_2), 4.02 - 4.06 (p, 1H, CH). ^{13}C NMR (101 MHz, Chloroform-d) δ 109.92, 75.87, 65.57, 63.11, 36.30, 34.70, 25.06, 23.93, 23.70. MS(ESI-TOF$^+$) for $C_9H_{16}O_3$ $[M+H]^+$ found 173.1168, calcd 173.1172.

2.4. ^{1}H NMR spectra of subject-object interactions between Q[6] and acetone

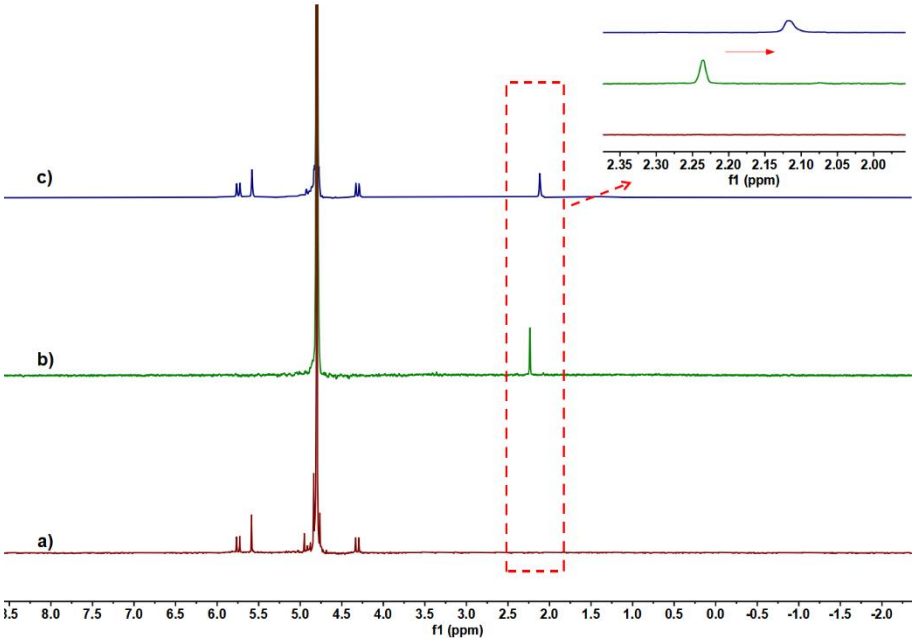

Fig. S2 ^{1}H NMR spectra (400 MHz, D_2O, pD = 7.0) recorded for (a) Q[6] (5×10^{-4} mol·L^{-1}); (b) acetone (5×10^{-4} mol·L^{-1}); and (c) $n_{acetone}$: $n_{Q[6]}$ = 1:1 and the enlarged views of the red rectangle.

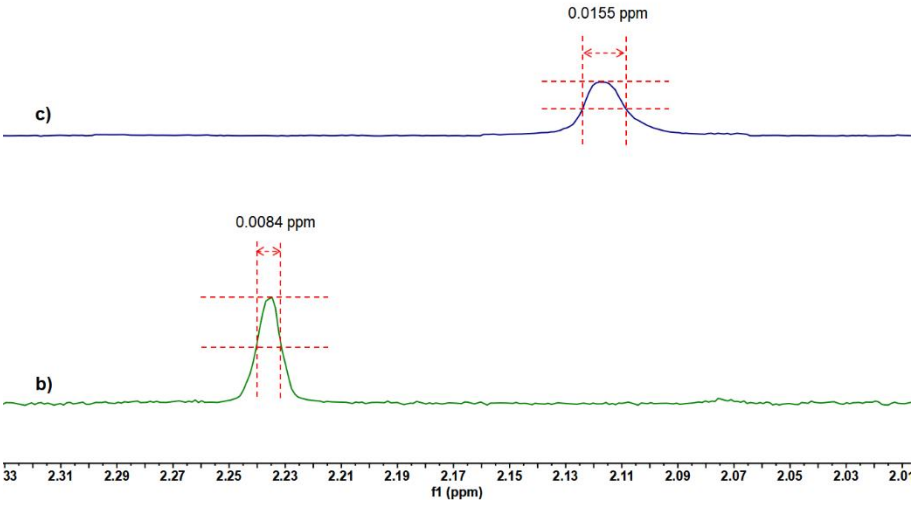

Fig. S3 The full width at half maximum (FWHM) of the partial enlarged view in Fig. S2: (b) acetone; (c) $n_{acetone}$: $n_{Q[6]}$ = 1:1.

2.5. HRMS spectra

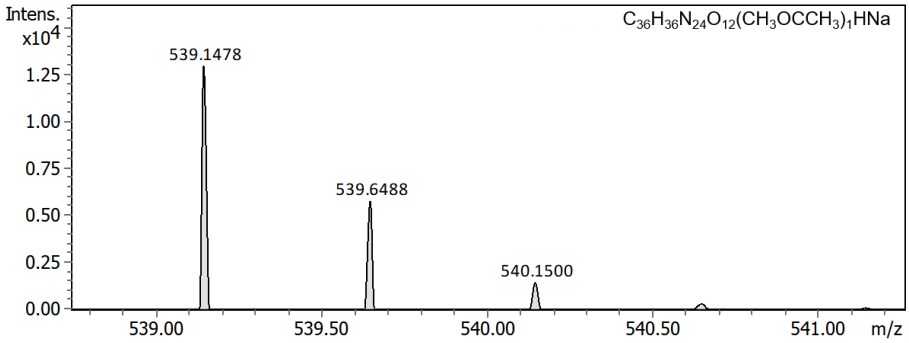

Fig. S4 The HRMS spectra of the acetone@Q[6] complex.

2.6. Comparative experiment

Table S3 Comparative experiments with different catalysts.

Catalyst	Solketal (% yield)
Q[5]	87%
Q[7]	69%
Para-Aminophenol (PAP)	--
PAP@Q[6]	--
Glycoluril	39.1
Glycoluril (18 wt%)	--

Reaction conditions: $n_{(gly)}$: $n_{(ace)}$ = 1:9, catalyst amount: 3 wt% $m_{(gly)}$, 50 °C, 20 min.

2.7 ^{1}H NMR spectra of Q[6] interacting with DDM and DDL subject-guest

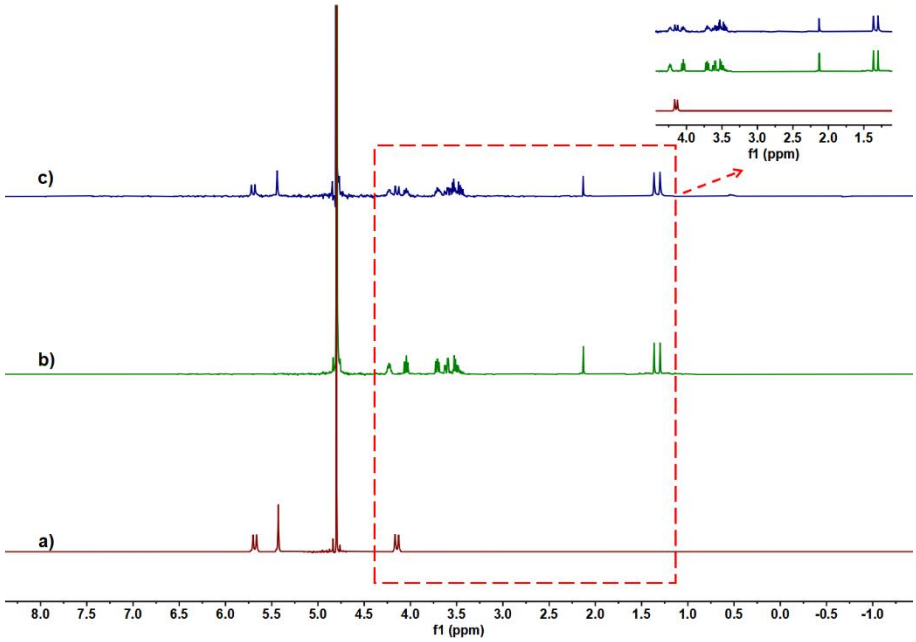

Fig. S5 ^{1}H NMR spectra (400 MHz, D_2O, pD = 7.0) recorded for (a) Q[6] (5×10^{-4} mol·L^{-1}); (b) DDM (5×10^{-4} mol·L^{-1}); and (c) n_{DDM} : $n_{Q[6]}$ = 1:1 and the enlarged views of the red rectangle.

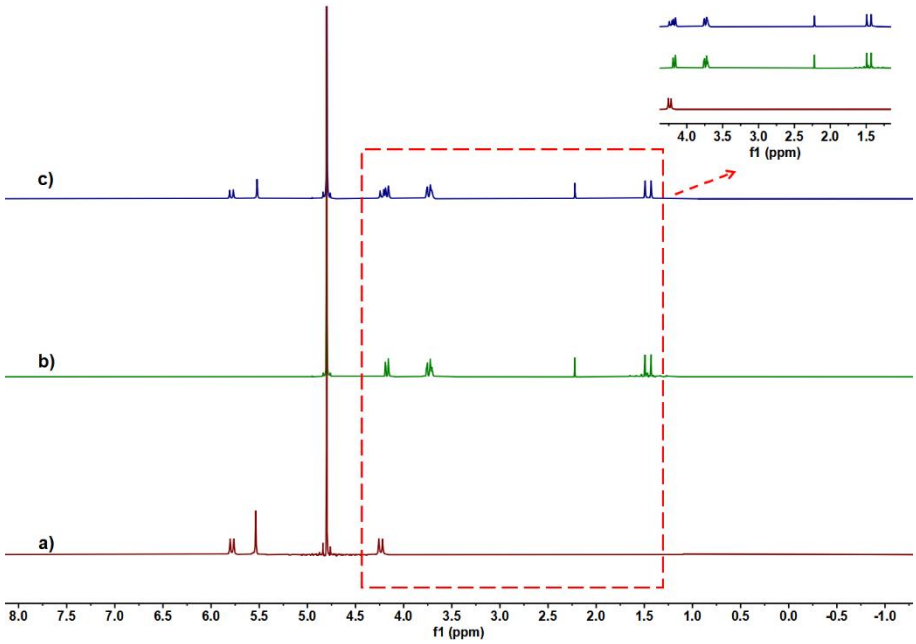

Fig. S6 ^{1}H NMR spectra (400 MHz, D_2O, pD = 7.0) recorded for (a) Q[6] (5×10^{-4} mol·L^{-1}); (b) DDL (5×10^{-4} mol·L^{-1}); and (c) n_{DDL} : $n_{Q[6]}$ = 1:1 and the enlarged views of the red rectangle.

3. Spectrum of the product

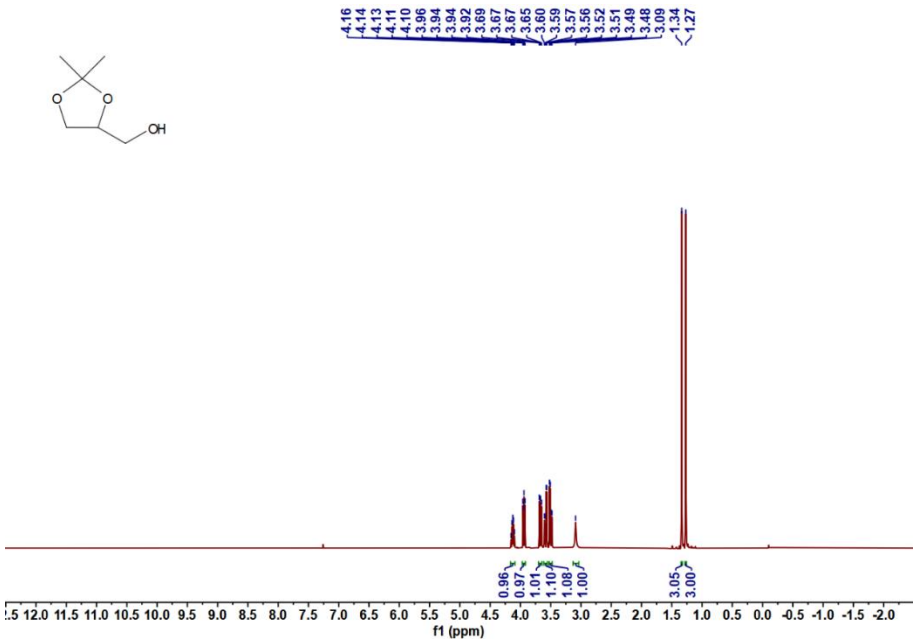

Fig. S7 ^{1}H NMR spectrum of DDM recorded in $CDCl_3$ at 400 MHz.

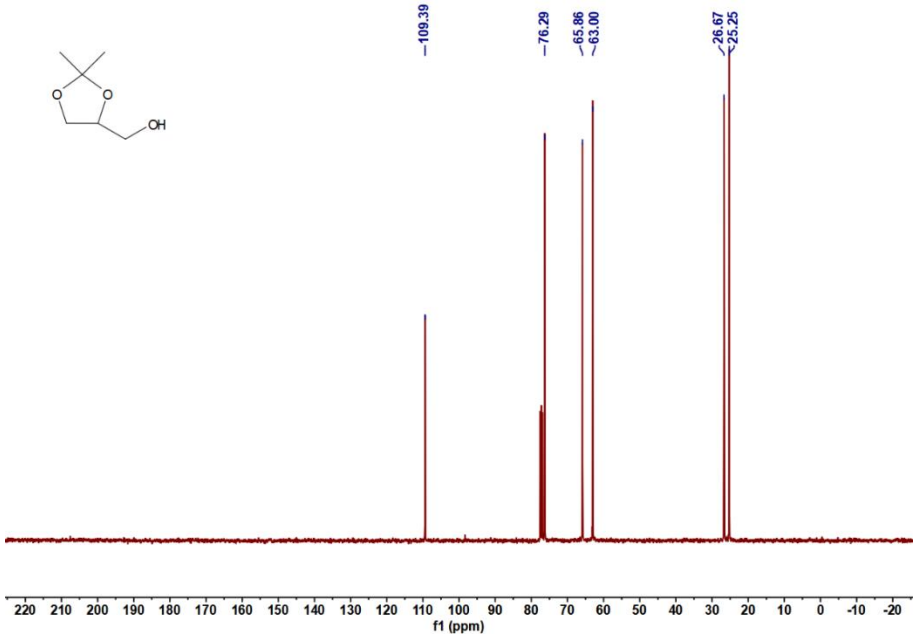

Fig. S8 ^{13}C NMR spectrum of DDM recorded in $CDCl_3$ at 101 MHz.

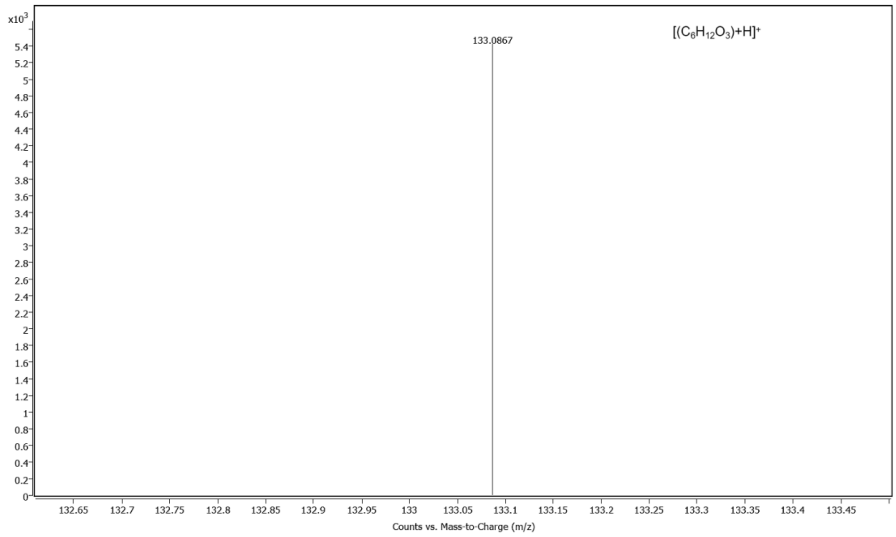

Fig. S9 HRMS spectra of DDM.

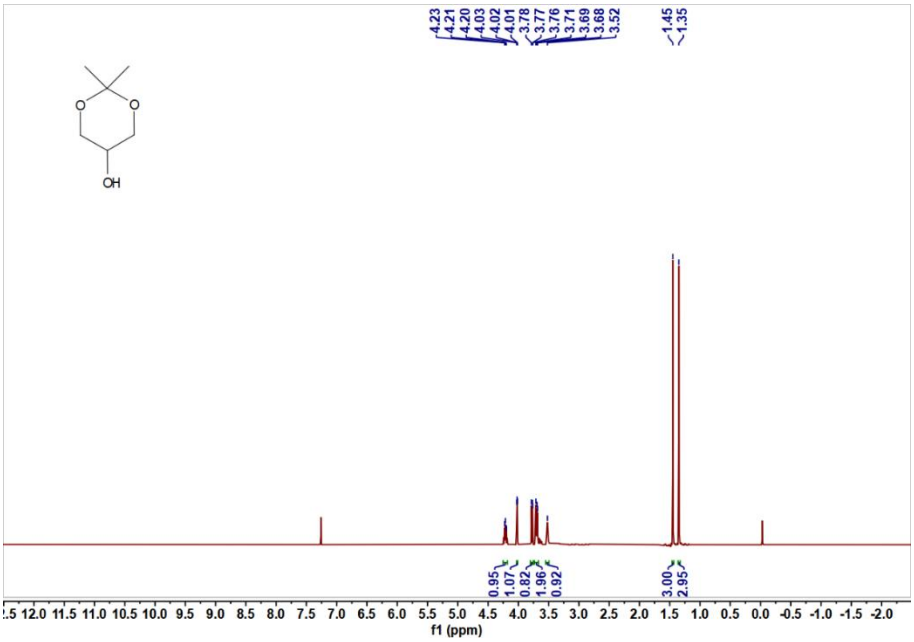

Fig. S10 ^{1}H NMR spectrum of DDL recorded in $CDCl_3$ at 400 MHz.

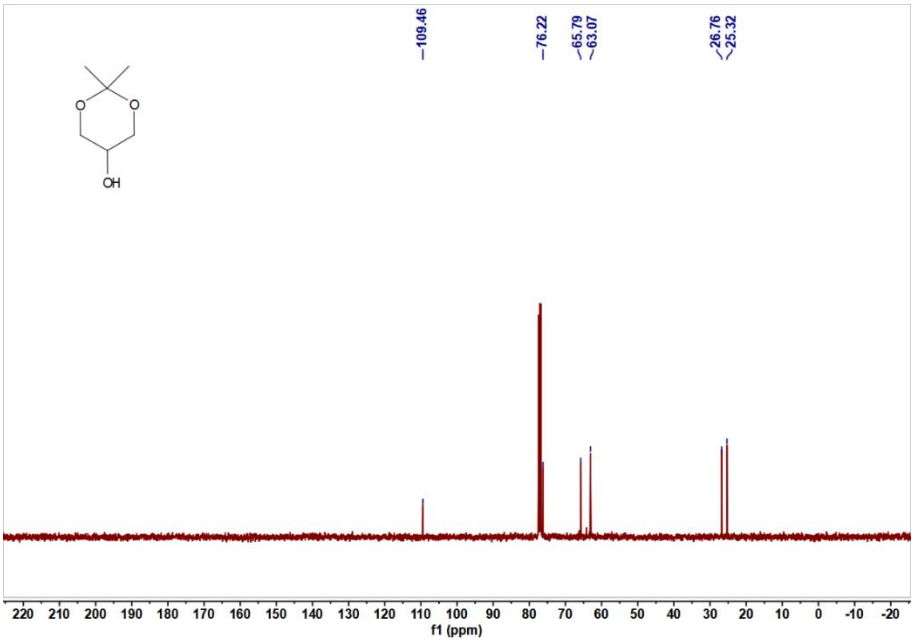

Fig. S11 ^{13}C NMR spectrum of DDL recorded in $CDCl_3$ at 101 MHz.

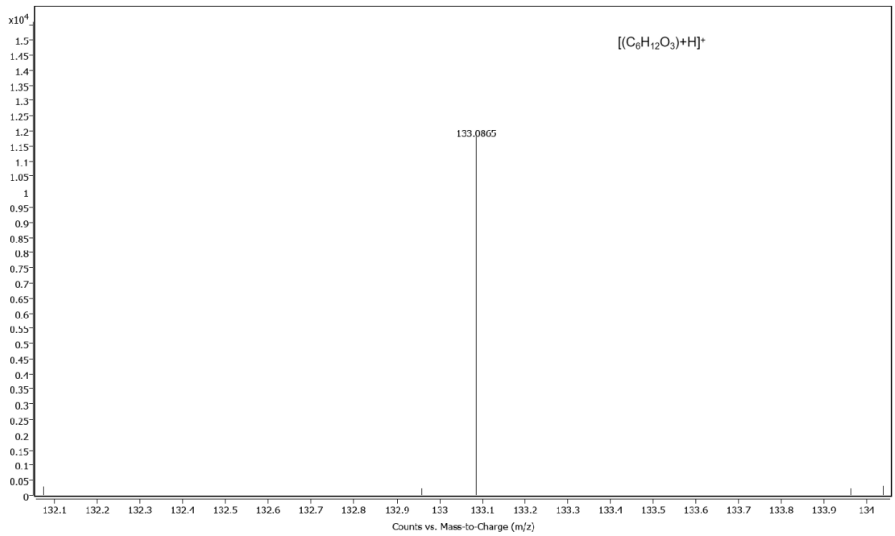

Fig. S12 HRMS spectra of DDL.

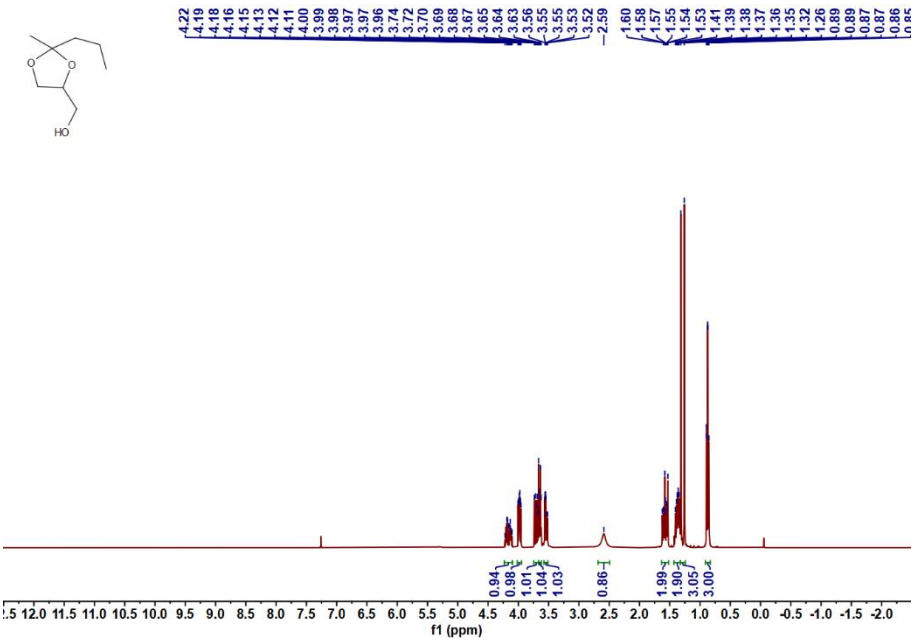

Fig. S13 ^{1}H NMR spectrum of 1a recorded in $CDCl_3$ at 400 MHz.

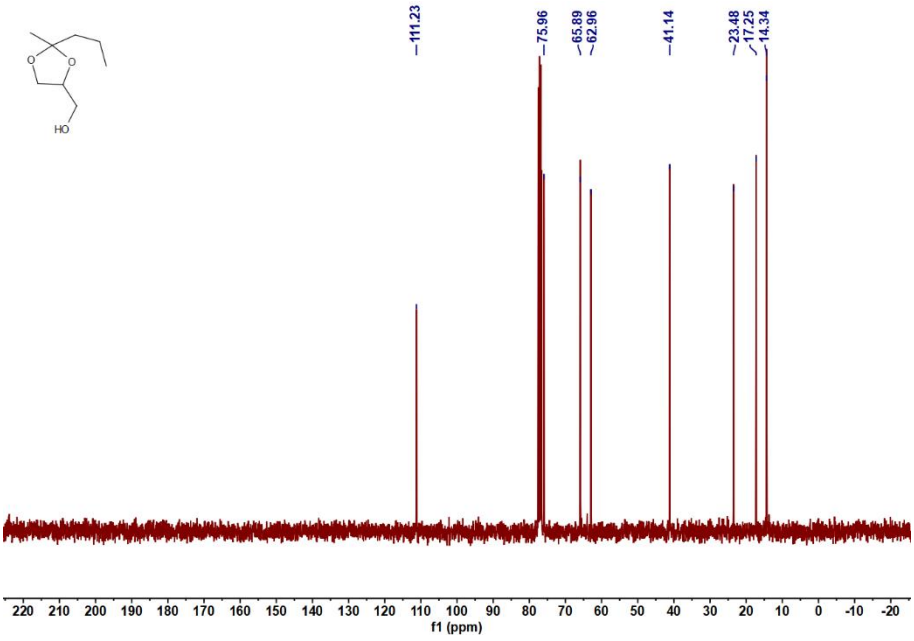

Fig. S14 ^{13}C NMR spectrum of 1a recorded in $CDCl_3$ at 101 MHz.

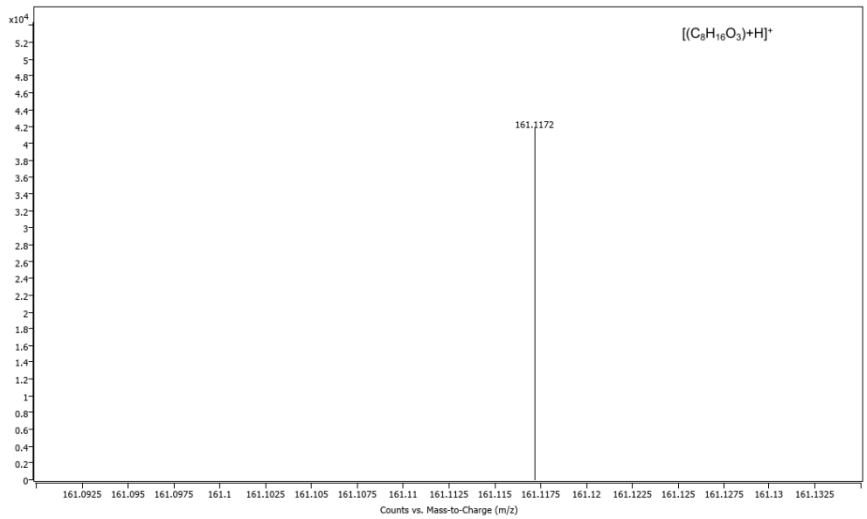

Fig. S15 HRMS spectra of 1a.

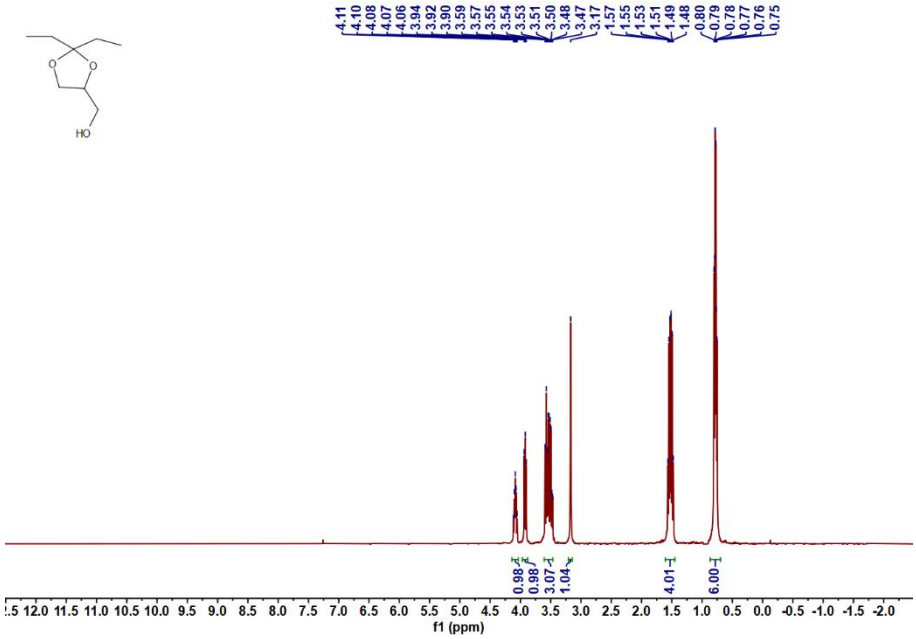

Fig. S16 ^{1}H NMR spectrum of 2a recorded in $CDCl_3$ at 400 MHz.

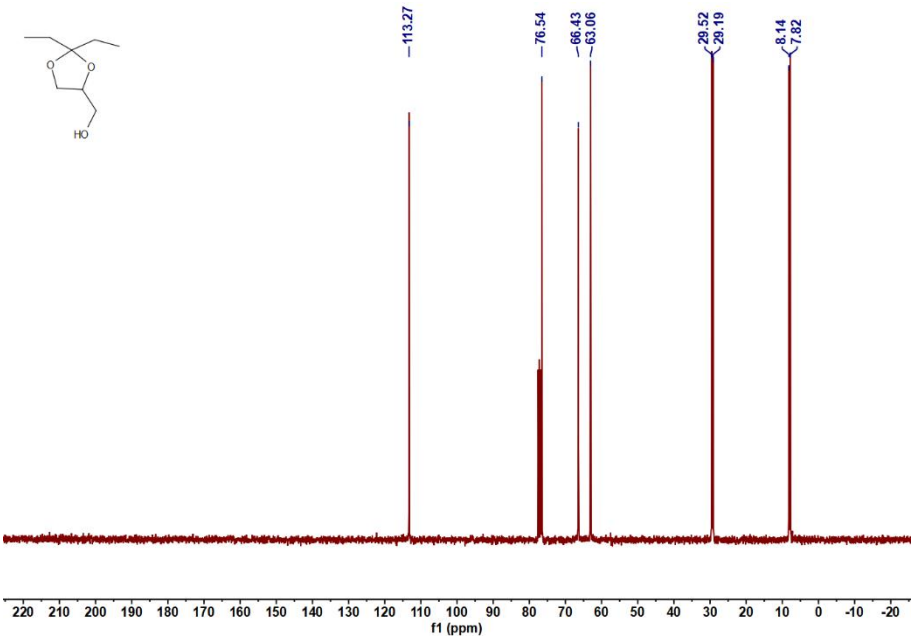

Fig. S17 ^{13}C NMR spectrum of 2a recorded in $CDCl_3$ at 101 MHz.

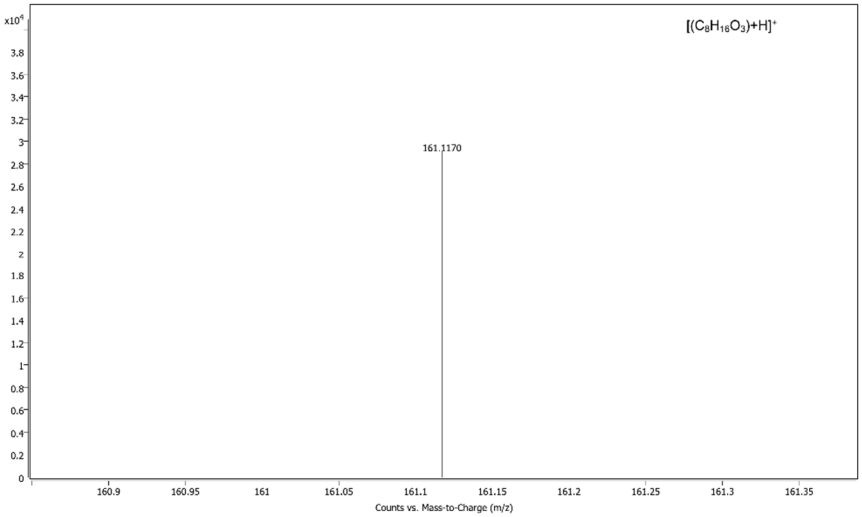

Fig. S18 HRMS spectra of 2a.

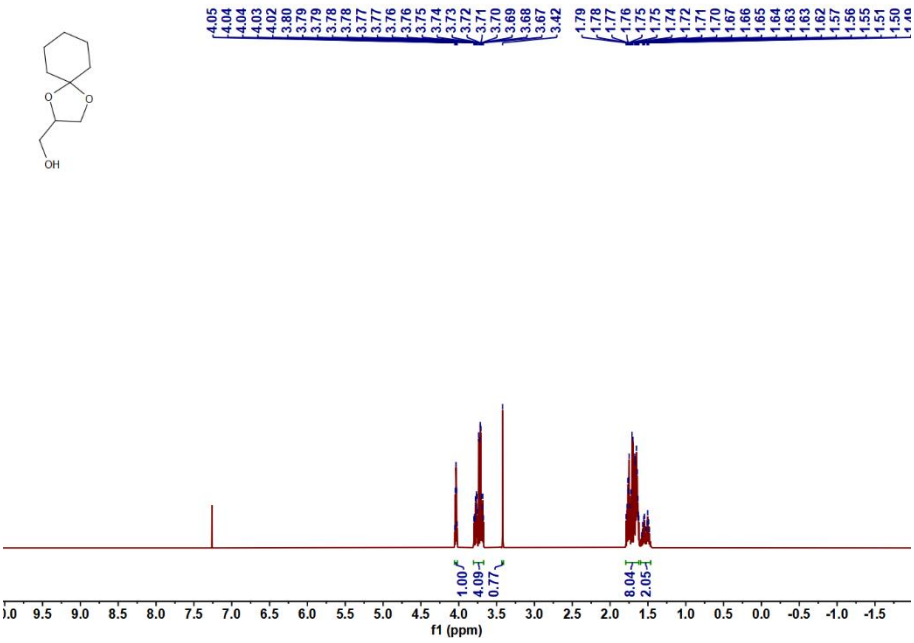

Fig. S19 ^{1}H NMR spectrum of 5a recorded in $CDCl_3$ at 400 MHz.

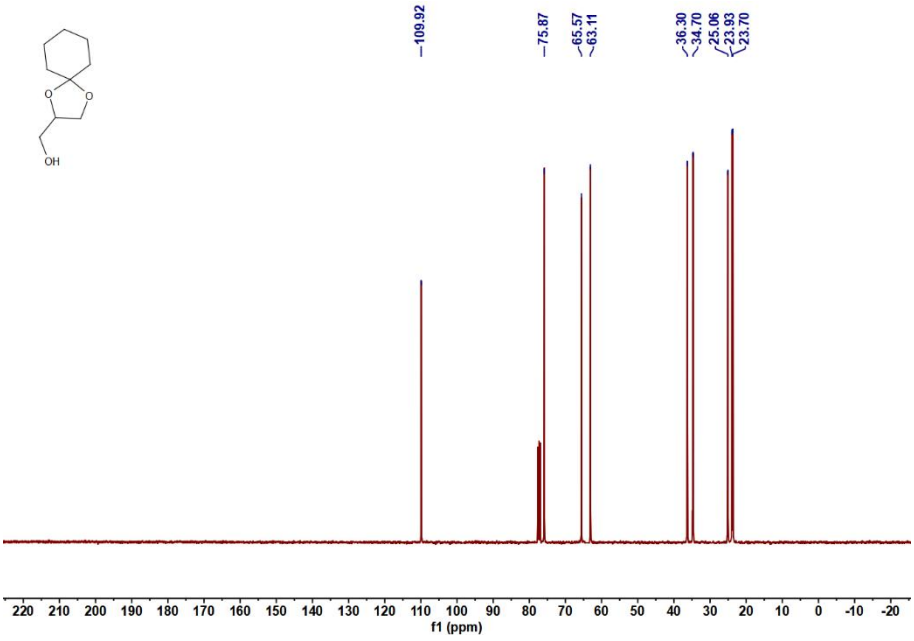

Fig. S20 ^{13}C NMR spectrum of 5a recorded in $CDCl_3$ at 101 MHz.

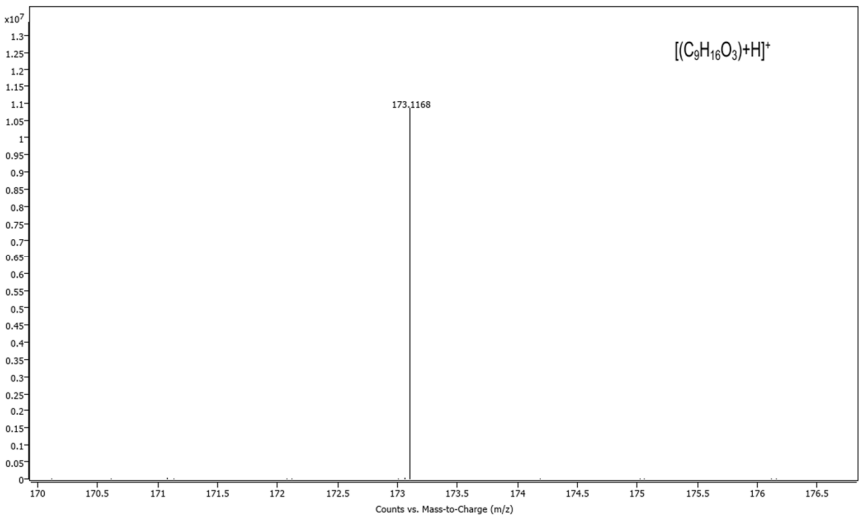

Fig. S21 HRMS spectra of 5a.

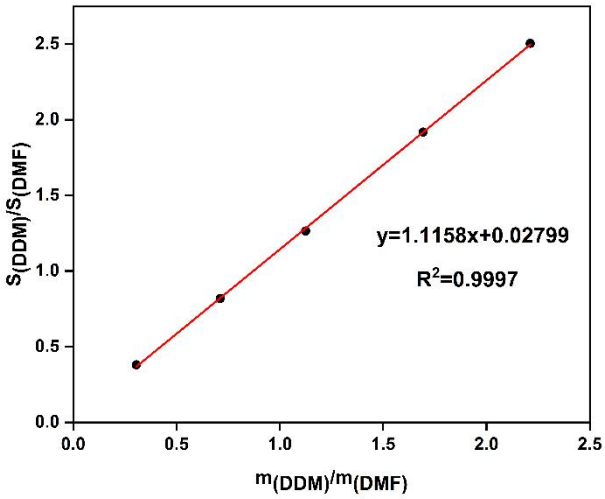

Fig. S22 DDM standard curve graph.

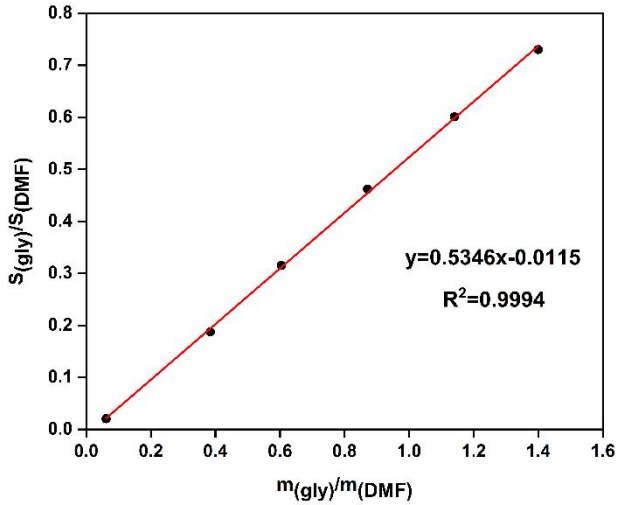

Fig. S23 Glycerol standard curve graph.

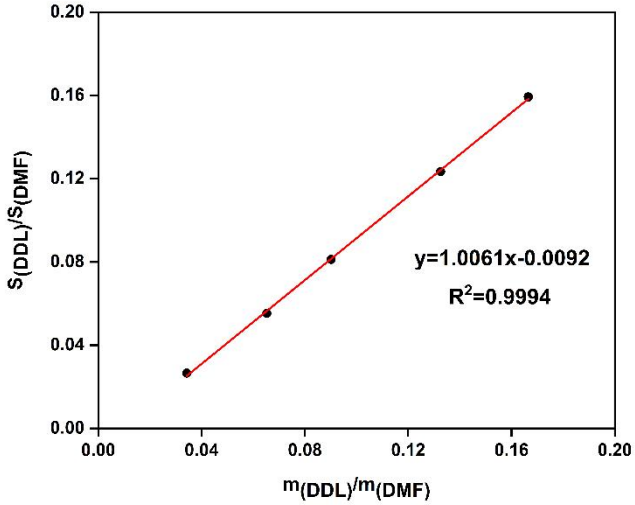

Fig. S24 DDL standard curve grap.

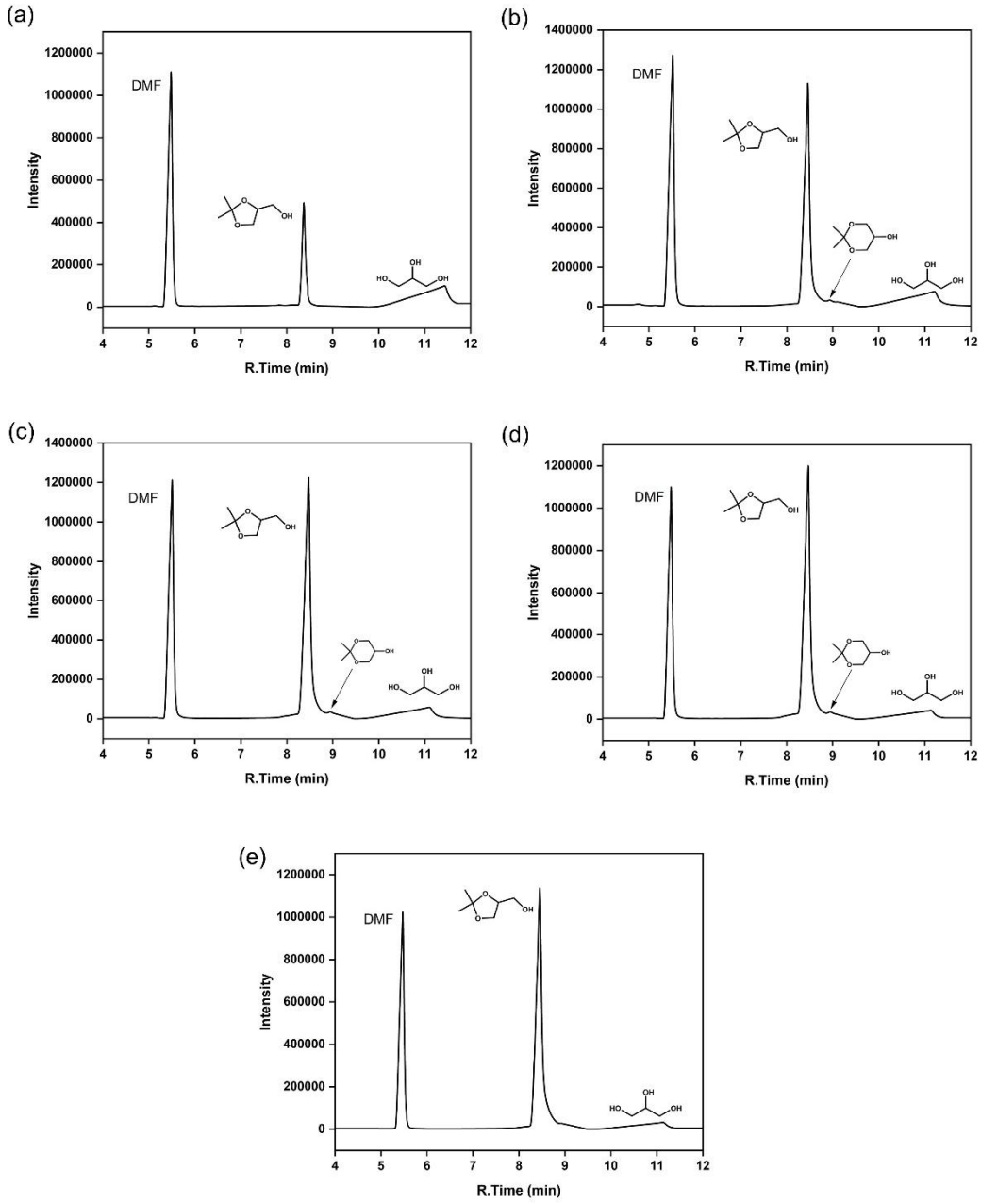

Fig. S25 GC plots of glycerol at different molar ratios to acetone: (a) 1:1; (b) 1:3; (c) 1:6; (d) 1:9; (e) 1:11.

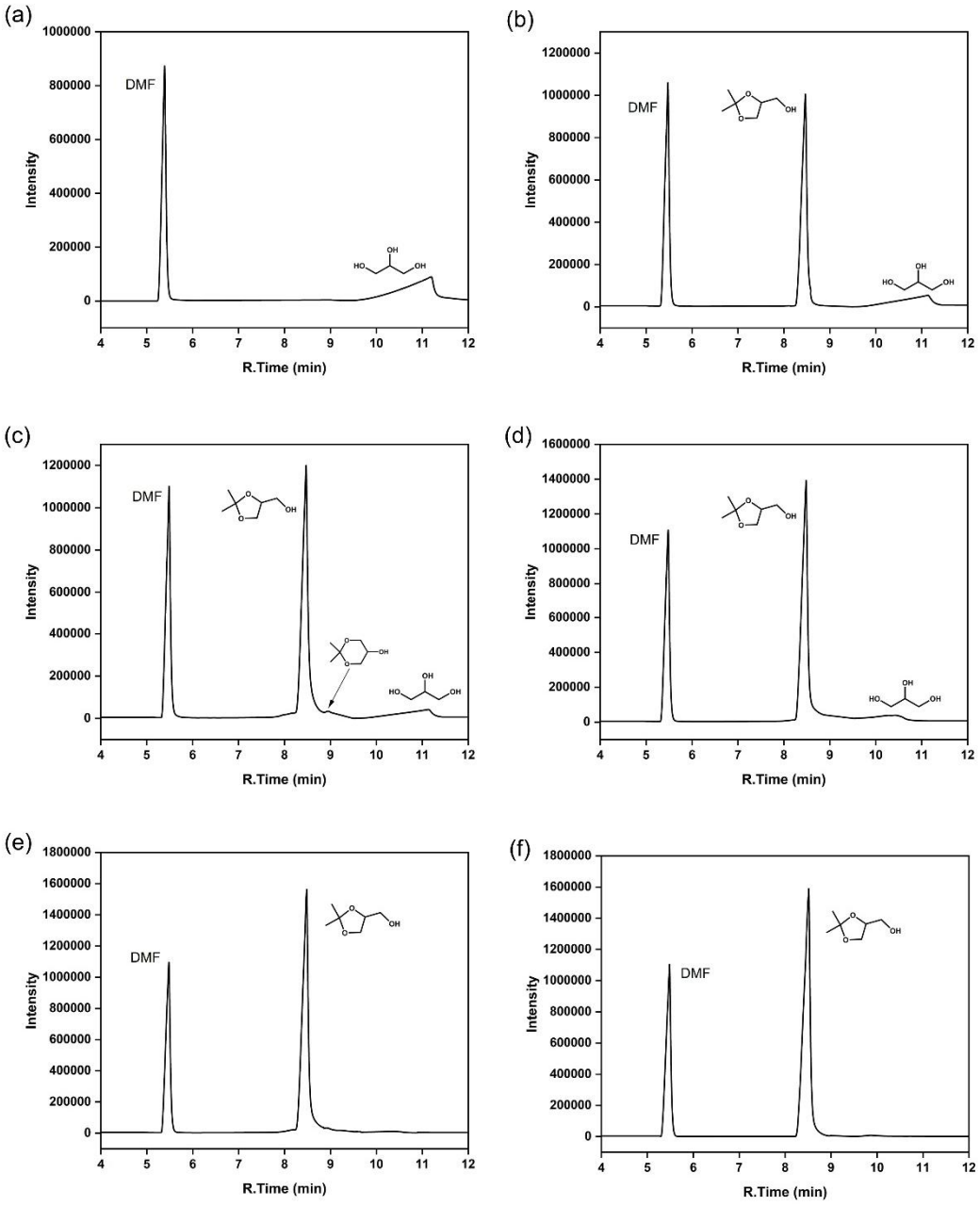

Fig. S26 GC plots at different catalyst dosages: (a) 0 wt% $m_{(gly)}$; (b) 0.5 wt% $m_{(gly)}$; (c) 1 wt% $m_{(gly)}$; (d) 2 wt% $m_{(gly)}$; (e) 3 wt% $m_{(gly)}$; (f) 4 wt% $m_{(gly)}$.

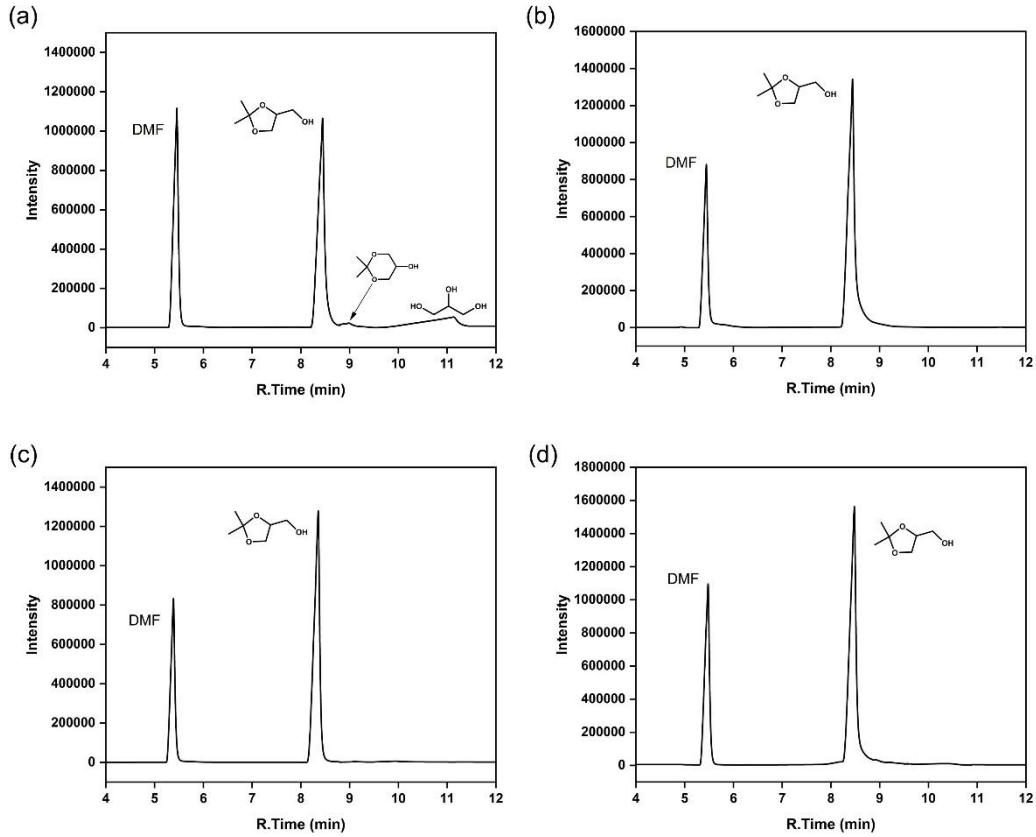

Fig. S27 GC plots at different reaction times: (a) 10 min; (b) 20 min; (c) 30 min; (d) 40 min.

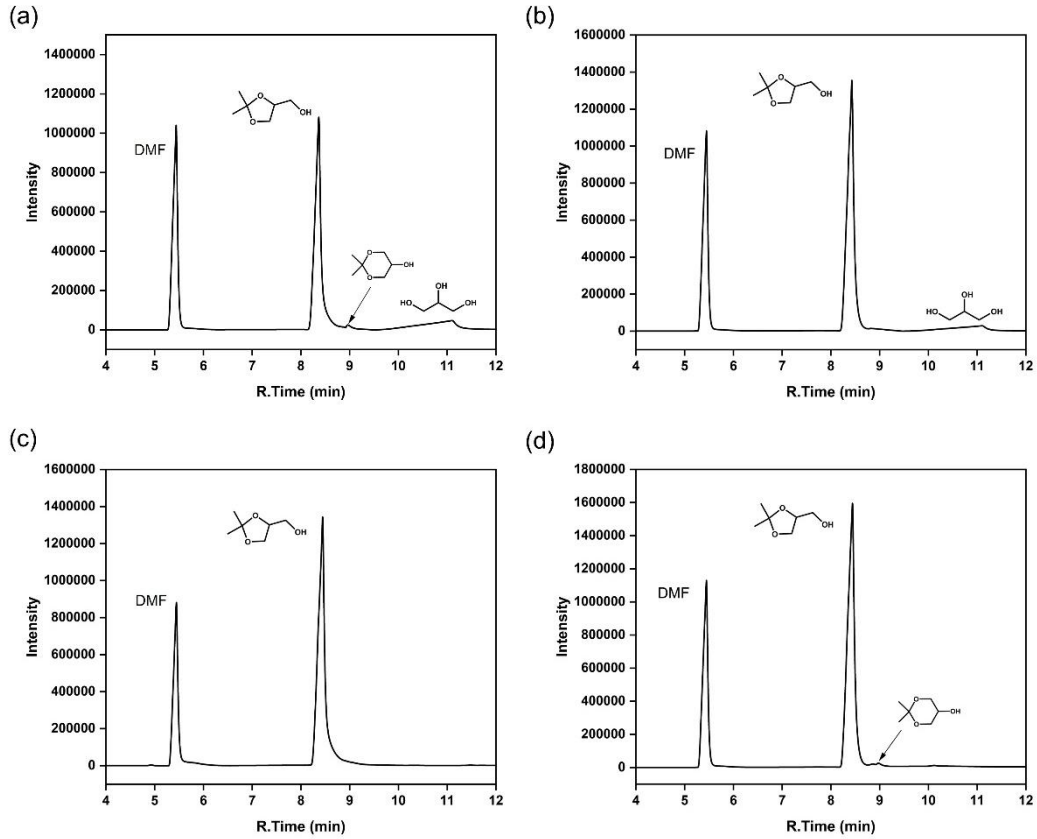

Fig. S28 GC plots at different reaction temperatures: (a) 25 ℃; (b) 40 ℃; (c) 50 ℃; (d) 70 ℃.

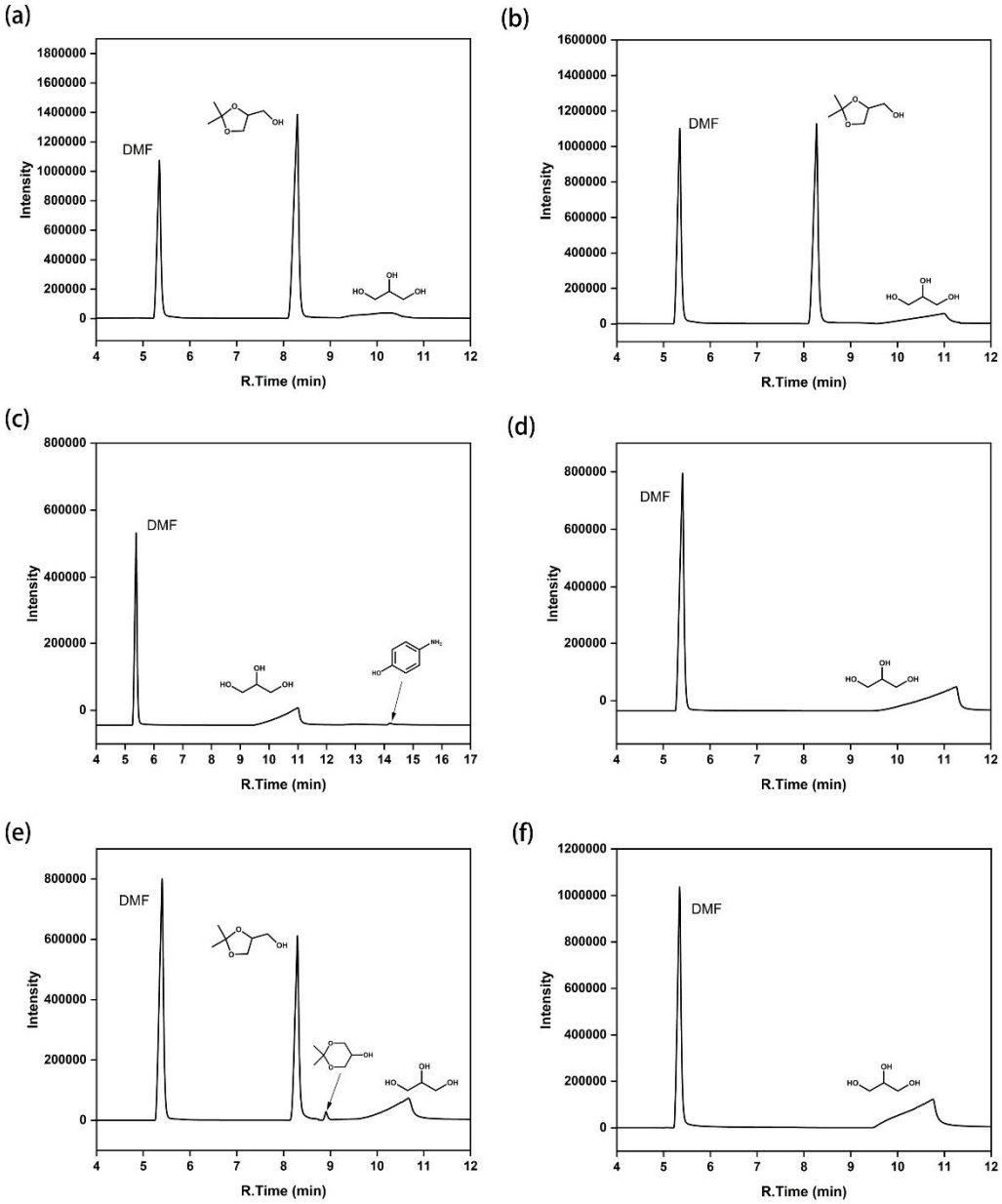

Fig. S29 Comparison experiment corresponding GC plots: (a) Q[5]; (b) Q[7]; (c) PAP; (d) PAP@Q[6]; (e) Glycoluril; (f) Glycoluril (18 wt%).

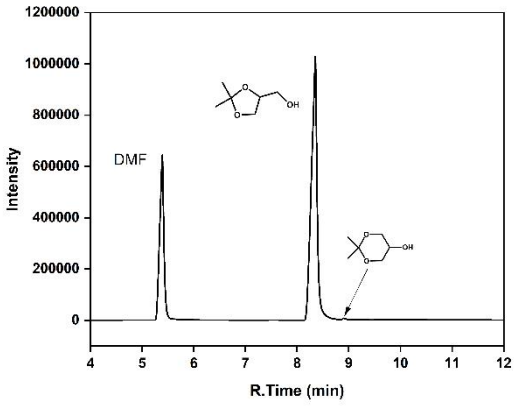

Fig. S30 GC diagram of enlargement the reaction.

4. References

1. O. Zbruyev, K. Belikov, S. Khimchenko, T. Blank and V. A. Chebanov, *Org. Process Res. Dev.*, 2022, **27**, 129-135.
2. X. Li, Y. Jiang, R. Zhou and Z. Hou, *Appl. Clay Sci.*, 2019, **174**, 120-126.
3. W. Wang, X. Zeng, Y. Dang, P. Ouyang, H. Zhang, G. Jiang, F. Dong, T. Yang, S. L. Suib and Y. He, *Chin. Chem. Lett.*, 2022, **33**, 1346-1352.
4. B. Saini, A. P. Tathod, S. K. Saxena, S. Arumugam and N. Viswanadham, *ACS Sustain. Chem. Eng.*, 2022, **10**, 1172-1181.
5. Y. Jiang, R. Zhou, B. Ye and Z. Hou, *J. Ind. Eng. Chem.*, 2022, **110**, 357-366.
6. K. Ravi and A. V. Biradar, *Fuel*, 2022, **321**, 124008.
7. A. Cheruvathoor Poulose, M. Medveď, V. R. Bakuru, A. Sharma, D. Singh, S. B. Kalidindi, H. Bares, M. Otyepka, K. Jayaramulu, A. Bakandritsos and R. Zbořil, *Nat. Commun.*, 2023, **14**, 1373.
8. T. Zhang, X. Xin, S. Liao, H. Liu, Y. Yu and B. Xu, *ChemistrySelect*, 2023, **8**, e202205005.
9. B. Matkala, S. Boggala, S. Basavaraju, V. S. Sarma Akella and H. P. Aytam, *Micropor. Mesopor. Mater*, 2024, **363**, 112830.
10. F. Mirante, P. Leo, C. N. Dias, L. Cunha-Silva and S. S. Balula, *Materials*, 2023, **16**, 7023.
11. R. Li, H. Li, P. Wang, Z. Wei, Z. Yin and Z. Wang, *Ind. Crops Prod.*, 2024, **221**, 119345.
12. R. K. Singh, V. Gosu and V. Subbaramaiah, *Biomass Bioenergy*, 2025, **193**, 107553.
13. A. Sharma, Ř. David, S. Srivastava, V. R. Hathwar, S. Siddhanta, M. Otyepka and K. Jayaramulu, *Appl. Mater. Today*, 2025, **45**, 102805.
14. L. Wang, D. Ren, J. Lang, K. Gao, X. Du, Y. Yang and Z. Huo, *J. Catal.*, 2025, **446**, 116084.
15. R. D, B. Saad, M. Mridul, S. L. Rokhum and G. Halder, *Chem. Eng. J.*, 2025, **514**, 163259.
16. R. K. Singh and V. Gosu, *Appl. Catal. A Gen.*, 2025, **703**, 120350.
17. D. Pan, J. Sun, H. Jin, Y. Li, L. Li, Y. Wu, L. Zhang and Z. Yang, *Chem. Commun.*, 2015, **51**, 469-472.
18. A. Mattarei, A. Rossa, V. Bombardelli, M. Azzolini, M. La Spina, C. Paradisi, M. Zoratti and L. Biasutto, *Eur. J. Med. Chem.*, 2017, **135**, 77-88.